Finite Element Analysis of Thin-Walled Square CFST Columns with Steel Lining Tubes Under Axial Compression

Xin Ye*

Chongqing University, Chongqing, China

*yxcqu1249787686@163.com

Abstract. This paper takes thin-walled square CFST columns with lining tube as the research object, aiming to conduct finite element analysis and parameter comparison on their axial compression performance. This member is a new type of composite column, with internal steel lining tubes and outer steel tubes connected by slot welds, which has the advantages of simplified manufacturing process and good constraint performance. To further investigate the mechanical performance of this member, Abaqus was used to conduct axial compression finite element numerical simulation on 18 short columns in this paper. Through parameter analysis, the influence of inner lining to outer pipe, inner pipe strength, external steel pipe strength, and concrete strength on the mechanical properties of components is discussed. The results show that the lin ing significantly increases the load carrying capacity of thin walled CFST columns, and also significantly improves the ductility of the parts. Meanwhile, as the strength of the internal and external steel pipes and the load carrying capacity of the parts increases, the strength of the concrete also significantly affects the mechanical properties of the components.

Keywords: Axial compression, thin-walled CFST, bearing capacity, ductility

1 Introduction

With the development of social economy, the construction industry has increasingly high structural requirements for buildings, and traditional concrete structures can no longer meet people's needs for safety, reliability, economy, and other aspects [1], Because of its light weight and high stiffness, thin-walled steel pipe concrete structure can improve the whole structure property of building, and it is widely applied in high building, bridge and large span building. However, thin-walled steel tube concrete structures have also encountered many problems during use, with the main problems being corrosion of the steel tube and cracking of the concrete. To solve these problems, researchers have started to study the technique of adding lining tube into thin-wall steel pipe concrete [2].

G. Zhao et al. (eds.), *Proceedings of the 2024 7th International Symposium on Traffic Transportation and Civil Architecture (ISTTCA 2024)*, Advances in Engineering Research 241,
https://doi.org/10.2991/978-94-6463-514-0_8

The technology of thin-walled steel tube reinforced concrete lining tube is to add steel sleeves to the steel tube concrete structure, forming a structural form of sleeve reinforcement [3]. This technology helps to control corrosion of steel tubes and cracking of concrete, and improve the load-bearing capacity and durability of thin-walled steel tube concrete structures. By using different forms and materials of lining tubes, optimizing the strength, stability, deformation ability, and other aspects of the components can further improve their performance. The method of stiffening ribs in this paper is to connect the inner circular lining tube with the outer steel tube through slot welds. ABAQUS is used to establish a finite element model and study the axial compression performance of the reinforced thin-walled square steel tube concrete short column with inner lining [4].

2 Model Design

The FEM model was designed for 18thin-wall square CFSTcolumns. The influence of the thickness ratio of the inner tube to the outer tube, the strength of the lining pipe, the strength of the outer pipe and the strength of the concrete on the axial compression of the thin wall rectangular CFST column were investigated. The cross section of the component is shown in Fig. 1, which is composed of three parts: outer steel pipe, concrete column, and steel lining tube. The specific parameters of the model are shown in Table 1.

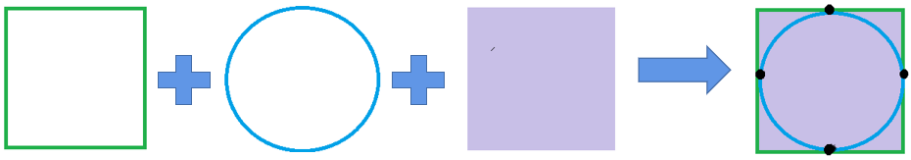

Fig. 1. Schematic diagram of member.

Table 1. Design parameters

No.[a]	Specimen	f_{yi}/Mpa[b]	f_{yo}/Mpa[c]	$f_{cu,k}$/Mpa	t_i/mm[d]	t_o/mm[e]	t_i/t_o	P (%)
1	SU-1		389	40		5.05		5.85
2	SC-1	389	389	40	2.83	2.83	1	5.85
3	SC-2	289	389	40	2.83	2.83	1	5.85
4	SC-3	339	389	40	2.83	2.83	1	5.85
5	SC-4	439	389	40	2.83	2.83	1	5.85
6	SC-5	489	389	40	2.83	2.83	1	5.85
7	SC-6	389	289	40	2.83	2.83	1	5.85
8	SC-7	389	339	40	2.83	2.83	1	5.85
9	SC-8	389	439	40	2.83	2.83	1	5.85
10	SC-9	389	489	40	2.83	2.83	1	5.85
11	SC-10	389	389	30	2.83	2.83	1	5.85

No.[a]	Specimen	f_{yi}/Mpa[b]	f_{yo}/Mpa[c]	$f_{cu,k}$/Mpa	t_i/mm[d]	t_o/mm[e]	t_i/t_o	P (%)
12	SC-11	389	389	35	2.83	2.83	1	5.85
13	SC-12	389	389	45	2.83	2.83	1	5.85
14	SC-13	389	389	50	2.83	2.83	1	5.85
15	SC-14	389	389	40	2.57	3.03	0.85	5.85
16	SC-15	389	389	40	2.32	3.23	0.72	5.85
17	SC-16	389	389	40	2.00	3.43	0.58	5.85
18	SC-17	389	389	40	1.81	3.63	0.5	5.85

a. The length of the designed member (L) is 1020 mm, the diameter of square steel tube (D) is 340 mm.The first specimen is a comparison specimen without a steel lining tube.

b. fyi refers to the yield strength of the steel lining tube, fyo refers to the yield strength of the outer steel tube.

c. ti refers to the thickness of the steel lining pipe, and to refers to the thickness of the outer steel tube.

3 Establishment of Numerical Model

3.1 Material Constitutive

The ABAQUS Plastic Damage Model is applied to the concrete, and the Equivalent Stress-Strain Relation is applied to the concrete properties. In the case of an inner lining reinforced sample, a circular section concrete model is used [5].

$$\xi = \frac{A_s f_y}{A_c f_{ck}} \tag{1}$$

$$\begin{cases} 2x - x^2 & (x \le 1) \\ \dfrac{x}{\beta_0 (x-1)^2 + x} & (x > 1) \end{cases} \tag{2}$$

Where: $x = \frac{\varepsilon}{\varepsilon_0}$; $y = \frac{\sigma}{\sigma_0}$; $\sigma_0 = f_c'$; $\varepsilon_0 = (1300 + 12.5 \cdot f') \cdot 10^{-6}$. σ_0 is the peak compressive stress of concrete, ε_0 is the corresponding peak compressive strain.

The steel (including outer steel tubes and lining tubes) adopts an ideal elastic-plastic model [6] [7]. The stress-strain relationship is as follows:

$$\sigma_s = \begin{cases} E_s \varepsilon & \varepsilon \le \varepsilon_y \\ f_y & \varepsilon \ge \varepsilon_y \end{cases} \tag{3}$$

Where: f_y is the yield strength of steel; Es is the elastic modulus of steel; ε_y is the

yield strain of the steel, $\varepsilon_y = \frac{f_y}{E_s}$.

3.2 Establishment of FEM Model

Among the main parameters of the plastic damage model of concrete [6, 7], the expansion angle is 40 degrees, the flow potential deviation is 0.1, fbo/fco is 1.16, the invariant stress ratio is 0.66667, and the viscosity coefficient is 0.0001; As shown in Figure 2，The core concrete adopts 8-node solid element C3D8R, and the steel tube and stiffener adopt shell element S4R.Through testing and comparing the accuracy of the grid, 30mm was ultimately used as the global grid size. Using a structured grid partitioning method, try to align the grid nodes of steel tubes, lining tubes, and core concrete as much as possible; The contact between the outer steel tube and concrete adopts surface to surface contact, with the concrete surface as the main surface and the inner surface of the steel tube as the secondary surface. The contact in the normal direction adopts "hard" contact, and the contact in the tangent direction adopts "penalty" friction, with a friction coefficient of 0.6; Between the lining tube and the concrete, a simulation method is adopted by embedding the lining tube into the concrete. To simulate the effect of slot weld, the corresponding slot welds positions of the lining tubes and outer tubes are connected by tying, with the lining tube as the main node; Establish rigid body constraints on the upper and lower end faces of the column and the reference point, set the column bottom as the fixed end, use displacement loading method, apply axial displacement to the upper reference point, and transfer the load to the model through the rigid surface [8-10].

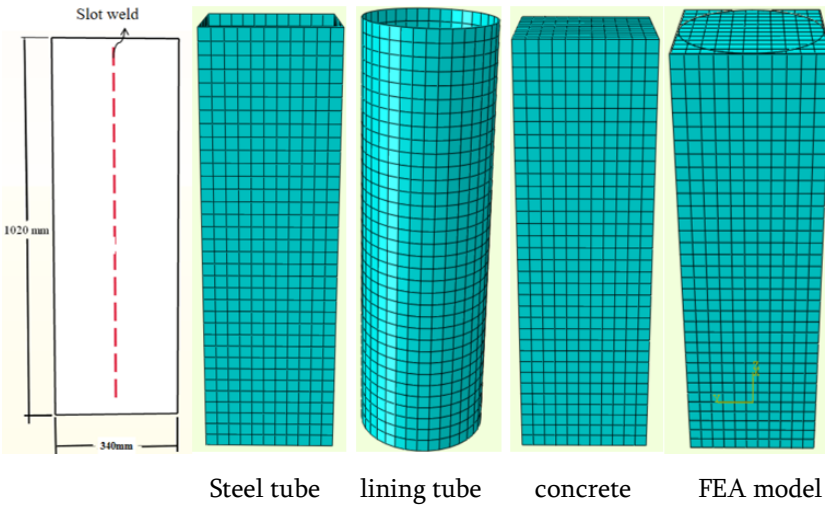

Fig. 2. Establishment of model.

4 Finite Element Analysis Results

For the purpose of analysing the stress evolution of the individual parts of the assembly, on the basis of a series of graphs (Figure 3-7) drawn on the basis of the finiteMeta-computing results, that is to say, the initial yield point of the steel pipe 1, the peak point 2, and the limit point 3 at which the load falls to 85% of the peak point load. Based on the SC-1 model, the stress evolution of steel pipe and concrete at every characteristic moment is introduced in detail.

At the initial yield point, the total stress on the core concrete is more uniform, and the corner stress is slightly higher. The stress variation of outer steel pipe is relatively small in the height range of the column, and the steel in the corner of the column is the first to yield. The stress distribution in cross section is relatively uniform, but its longitudinal stress is less than that of outer steel pipe.

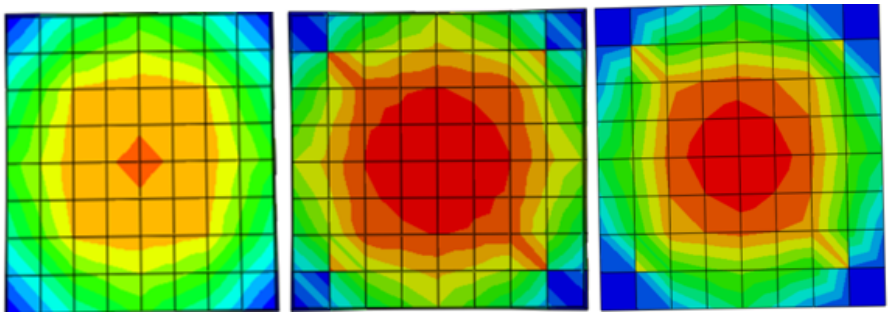

Fig. 3. Longitudinal stress in the cross-section of concrete columns

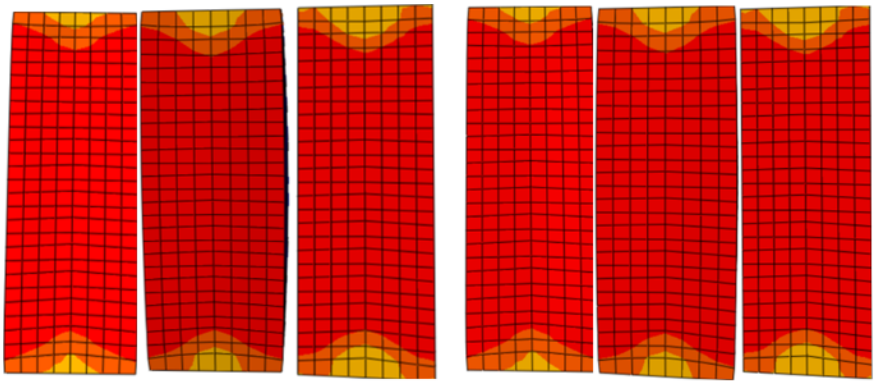

Fig. 4. Longitudinal stress of outer steel tube

Fig. 5. Circumferential stress of outer steel tube

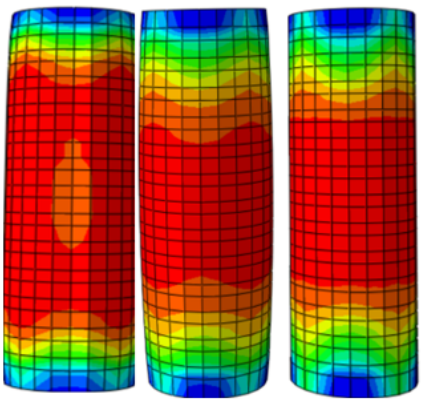

Fig. 6. Longitudinal stress of steel lining tubes

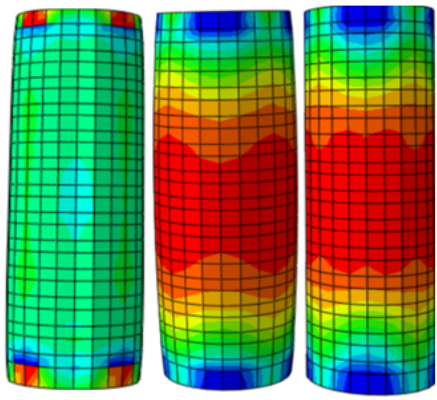

Fig. 7. Circumferentiall stress of steel lining tubes

At the peak, the longitudinal compressive stress in the cross section of the column is obviously higher than the original yield point, and there are many concentric circles in the stress distribution. The stress in core area and corners increases significantly. Most areas of the outer steel tube yield without significant buckling. Most of the areas of thelining tube yield, and there is a hysteresis effect of longitudinal stress along the cross section. The circumferential stress of the lining also increases significantly compared to the initial yield point.

At the limit point, the longitudinal stress pattern of the core is changed from circular to square, and the four side concrete is out of work. Nearly all external steel tubes yield, and there is obvious deformation near the center. The steellining tube almost completely fails.

5 Parameter Analysis

5.1 Strength of Outer Steel Tubes

Figure 8 illustrates the load-carrying curves of the members with different external steel tube stiffness. Compaying with thin wall CFST columns without lining, the bearing capacity of thin-wall CFST columns with liner pipe is significantly increased, and the ductility of the descending section is better. With the increase of the yield strength of the steel, the initial rigidity of the members does not change significantly, and the bearing capacity of the members is increased obviously. There is no significant change in the ductility of the descending segment.

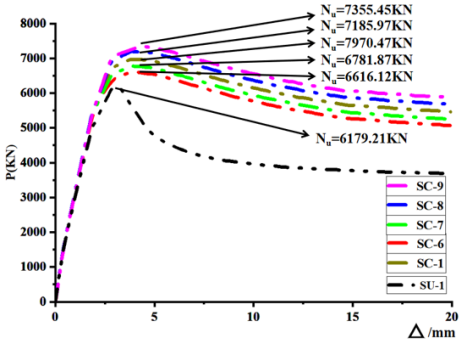

Fig. 8. Load-displacement curve under the influence of outer steel tube strength

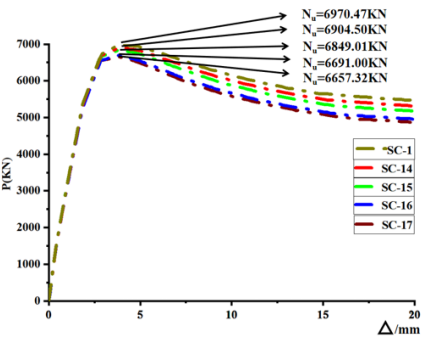

Fig. 9. Load-displacement curve under the influence of thickness ratio between liner and outer tube

5.2 Thickness Ratio of Liningr to Outer Tube

Figure 9 illustrates the load-displacement curves of components with different lining- and outer-tube thickness ratios. When the content of steel is constant, the thickness of lining pipe is larger, and the bearing capacity is larger. There is no significant change in the initial stiffness and ductility of the member duringingly.

5.3 Concrete Strength

Figure 10 illustrates the load displacement curve of the component with concrete strength as a variable. The ultimate bearing capacity of the composite column is increased by 6.48%, 6.02%, 5.96% and 5.38% for each 5 MPa. The initial stiffness of the component increases as the strength of the concrete increases, but the downward trend is steeper, which leads to a lower ductility of the component.

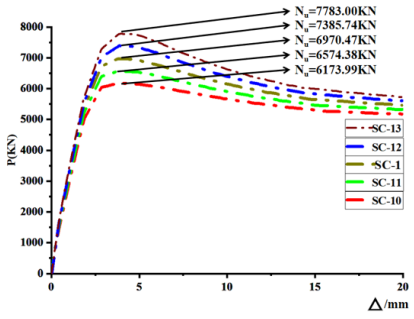

Fig. 10. Load-displacement curve under the influence of concrete strength

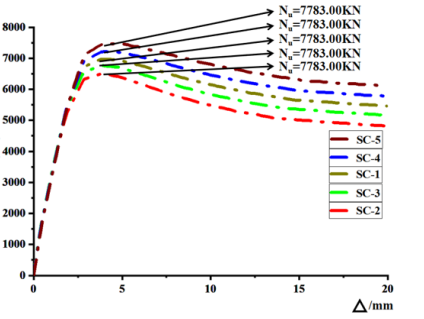

Fig. 11. Load-displacement curve under the influence of steel lining tubes strength

5.4 Steel Lining Tubes Strength

Figure 11 shows the load displacement curves of components withdifferent liner strength. As the yield strength of the steel lining tubesincreases, there is no significant change in the initial stiffness of the member. When the strength of the lining tube increases from 289 MPa to 489 MPa, thebearing capacity of each component significantly increases. There is nosignificant change in the ductility of the descending segment.

6 Conclusion

In this paper, a non-finite element method for the axial compressive properties of thin-wall rectangular concrete columns with circular liner is presented:

(1) Local buckling of thin-wall rectangular CFST columns is delayed by the reinforcement of circular lining tubes, which can effectively improve the axial performance of thin-walled rectangular CFST columns.

(2) For thin-walled square CFST columns with circular steel lining tubes, improving the strength of the inner and outer tubes as well as the strength of concrete can improve the ultimate bearing capacity of components, with concrete strength having the greatest impact on the ultimate bearing capacity. In addition, increasing the strength of concrete can also increase the initial stiffness of the component.

(3) When the steel content is constant, the ratio of the thickness of the lining tube to the thickness of the outer tube increases, and the ultimate bearing capacity of the member increases.

It should be noted that the results of this study and the proposed axial resistance model can be easily applied to thin walled CFST structures ($B/t \geqslant 80$). But the linerstiffened CFST columns with discontinuous slotweld can also be used in conventional thick CFST columns, which has the advantage of reducing welding-up while increasing confinement. Related research projects need to be further carried out.

References

1. Zheng Y, Zeng S. Design of L-shaped and T-shaped concrete-filled steel tubular stub columns under axial compression[J]. Eng. Struct, 2020(207):110262.
2. Lei M, Li Y Q, Luo J H, et al. Experimental and theoretical study on concrete-filled T-shaped steel tubular columns under uniaxial eccentric compression[J]. Eng. Struct., 2022(265):114531.
3. Lei M, Li Y L, Li Y Q, et al. Behavior of concrete-filled T-shaped steel tubular beam-columns under biaxial compressive loads[J]. Eng. Struct., 2023(277):115409.
4. Du G F, Zhang J, Li Y, et al. Experimental study on hysteretic model for L-shaped concrete-filled steel tubular column subjected to cyclic loading[J]. Thin-Walled Struct,

2019(144):106278.
5. Pagoulatou M, Sheehan T, Dai X. Finite element analysis on the capacity of circular concrete-filled double-skin steel tubular (CFDST) stub columns[J]. Engineering Structures, 2014(72):102-112.
6. C L G, W C B, J Y Z, et al. Experimental and numerical behavior of eccentrically loaded square concrete-filled steel tubular long columns made of high-strength steel and concrete[J]. Thin-Walled Structures, 2021(159):107289.
7. Ji J, Yang M, Jiang L. Output-only parameters identification of earthquake-excited building structures with least squares and input modification process[J]. Applied Sciences, 2019,9(4):696.
8. Lam L, Teng J. Design-oriented stress–strain model for FRP-confined concrete[J]. construction and building materials, 2003(17):471-489.
9. Zheng Y Q, Zeng S X. Flexural behaviour of stiffened and multi-cell L-shaped CFSTs considering different loading angles[J]. J. Constr. Steel Res., 2021(178).
10. X D F, R L D, Y B, et al. Comparative study of square stirrup-confined concrete-filled steel tubular stub columns under axial loading [J]. Thin-Walled Structures, 2016(98):443-453.